J Mater Sci (2006) 41:7361–7373
DOI 10.1007/s10853-006-0794-0

Effect of 0.1% vanadium addition on precipitation behavior and mechanical properties of Al-6063 commercial alloy

S. Camero · E. S. Puchi · G. Gonzalez

Received: 17 March 2005 / Accepted: 6 December 2005 / Published online: 19 September 2006
© Springer Science+Business Media, LLC 2006

Abstract The effect of 0.1 wt% vanadium additions on the precipitation behavior and the mechanical properties of a commercial Al-6063 alloy were studied. A master alloy containing 3 wt% V was added during casting. The cast ingot was homogenized, extruded and cooled employing two different cooling modes: forced air and water. Further aging was carried out following the standard T5 and T6 treatments for alloys with and without vanadium. The microstructural characterization, mechanical properties, and fractografic study were carried out. The addition of 0.1% vanadium to Al-6063 alloy under T5 treatment, accelerates the precipitation kinetics of β'' and β' phases. The alloys with and without vanadium under T6 show a similar behavior, the co-existence of β' and β'' precipitation is observed in both alloys. In general, vanadium additions to Al 6063 have a detrimental effect on the mechanical properties, showing only a beneficial effect for certain specific conditions.

S. Camero · E. S. Puchi
Escuela de Metalurgia y Ciencia de los Materiales, Facultad de Ingeniería, Universidad Central de Venezuela, Caracas, Venezuela

S. Camero
e-mail: soniacamero@cantv.net

G. Gonzalez (✉)
Laboratorio de Ciencia e Ingeniería de Materiales, Dpto. Ingeniería, Instituto Venezolano de Investigaciones Científicas, aptdo. 21827, Caracas 1020-A, Venezuela
e-mail: gemagonz@ivic.ve

Introduction

The Al series 6000 alloys is one of the most important groups of alloys for the extrusion of plates, rods, tubes, bars, and other shapes. These alloys have good formability and corrosion resistance with medium strength and very good surface finish. They contain silicon and magnesium in the appropriate proportions to form magnesium silicide, thus making them heat treatable by applying T5 temper and reach full properties with an additional T6 artificial aging. The most widely used Al-extrusion alloys for structural applications is AA 6063 with the range of composition shown in Table 1 [1]. The major alloying elements are silicon and magnesium, while the elements like Cu, Mn, Cr, Ti and Zn may be present in the alloy below the specified maximum limits. The maximum permissible limit of Fe, one of the most common impurity in Al alloys, is also shown in Table 1. Although the impurity elements are restricted to small amounts (~0.1 wt%), such impurities could have substantial effects on the mechanical properties of these alloys [2–4].

The precipitation behavior of Al–Mg–Si alloys has been extensively studied [5–20]. The precipitation sequence has been proposed as follows: supersaturated (SSSS) → cluster → metastable β'' → metastable β' → stable β. Recent studies [13–19] have proposed a modification in this sequence consisting of: Al (SSSS) → cluster of Si atoms and clusters of Mg atoms → dissolution of Mg clusters → formation of Mg/Si co-clusters → small precipitates of unknown structure → β'' precipitates → β' and β'' precipitates → β Mg_2Si.

The formation of clusters of solute atoms have been proposed to explain indirect observations of precipitation through thermal analysis [12, 20] and

Table 1 Chemical compositions of 6063 aluminum (wt.%)

Si	Mg	Fe	Cu	Mn	Cr	Ti	Zn	Al
0.2–0.6	0.45–0.9	0.35	0.10	0.10	0.10	0.10	0.10	bal.

electrical resistivity [9, 24]. However, uncertainties exist on the mechanisms and crystal structure of the precipitates formed. Edwards et al. [15] reported a detailed study to clarify the precipitation sequence, the crystal structure and compositions of the precipitating phases using differential scanning calorimetry (DSC), atom probe field ion microscopy (APFIM) and high-resolution dark field electron microscopy (HRDFEM). They found that the precipitation sequence is as follows: independent clusters of Mg and Si atoms → co-clusters that contain Mg and Si atoms → small precipitates of unknown structures → β'' needle-shape precipitates → β' lath-shaped precipitates and β'' rod shape precipitates → β (Mg_2Si). They proposed a new base-centered monoclinic structure for β'' precipitates based on high-resolution images. Muruyama et al. [19] characterized the formation of small co-clusters and precipitates in Al–Mg–Si with balanced and excess Si during natural and artificial aging. They suggested that a low density of β'' precipitates with natural aging indicate that co-clusters were reverted, at the temperature for artificial aging, resulting in reduced precipitation kinetics.

The effects of small amounts of alloy additions of Cr, Mn and Zr to Al–Mg–Si alloys have been studied [25, 26]. These additions act as dispersoid forming elements and affect advantageously the strength and toughness of these alloys. Also, Cu additions up to 0.3 wt% on balanced and excess Si alloy have a refining effect on the Mg_2Si precipitates, increasing the strength without a lost in ductility. The formation of dispersoids containing Mn and/or Cr in Al–Mg–Si alloys was studied by Lodgaard and Ryum [27] placing special emphasis on the nucleation mechanisms.

There are very few reports on the effect of vanadium as a minor addition to Al 6063. Schwellinger et al. [28] found that vanadium additions to Al–Mg–Si alloys improved the formation of fine recrystallized grain, enhancing the mechanical properties combination. On the other hand, Babic et al. [29] reported an increase on hardening with vanadium additions higher than 0.2%wt, while Mondolfo [30] found that even after heat treatments no effect on hardening was observed with vanadium additions.

Although extensive studies exist on the precipitation sequence and mechanical properties of the Al 6063 alloy, a systematic study of the effect of vanadium as a minor addition on the precipitation behavior and the mechanical properties of this alloy has not been reported.

The purpose of this work is to study the influence of a small addition of vanadium on the recrystallization behavior, precipitation behavior and the mechanical properties of the alloy 6063. Forced air-cooling post solution treatment was additionally carried out in order to examine the effectiveness of vanadium to restrict recrystallization and grain growth in the alloy.

Experimental

Aluminum of commercial purity (99.77 wt%) was melt in a gas furnace at 750 °C for 8 h. The alloying elements were added in the form of Master alloys: vanadium (3 wt%), silicon (20 wt%), manganese (5 wt%) and magnesium (10 wt%). Agitation was performed for 5 min every half an hour during 4 h. The casting was carried out in an iron crucible and then air cooled. Ingots of 15 cm diameter and 60 cm length were obtained. Al 6063 without vanadium was prepared using the same conditions.

The ingots were homogenized at 580 °C for 7 h in a batch furnace and cooled to room temperature using forced air at a cooling rate of 300 °C/h. The homogenized ingots pre-heated at 470 °C during 10–15 min were extruded in a 1650 T horizontal hydraulic press with a press exit temperature of 495 °C. The extruded rectangular shape pieces (15 cm wide, 1.5 cm thick) were cooled down to room temperature following two cooling modes: forced air and water quench. A part of the batch (with and without vanadium) was stretched and artificially aged at the plant conditions 175 °C for 8 h (T5) with previous natural aging of 24 h. The other part was aged at the laboratory scale following a T6 aging scheme as follows: extrusion ingots were cut in square sections 2 cm × 2 cm × 1.5 thick. Groups of 10 samples were solution treated at 580 °C for 1 h and cooled to room temperature following two cooling modes: air and water quench. For both cases the samples were natural aged for 24 h at room temperature, previous to the artificial ageing treatments. Artificial aging treatments were performed by immersion in an oil bath at 175, 250 and 325 °C for periods between 1 min and 128 h and air cooled to room temperature. These samples were stored at low temperature until further analysis was performed.

The chemical compositions of the alloys studied are shown in Table 2. The samples were metallographically prepared for optical observation and hardness measurements. Vickers hardness was carried out using a load of 5 kg and at least 10 measurements were taken for each sample. X ray analysis were carried out in the as-cast, homogenized and aged T5 and T6 samples with and without vanadium, using Cu K_α radiation. The samples were characterized in a Philips 505 scanning and EM 420 transmission electron microscopes equipped with energy dispersive X-ray spectrometers. The specimens for transmission electron microscopy were electropolished by doubled jet technique. The electrolyte was 20% perchloric acid in 80% methanol using 15 V and 0.1 A and a temperature of –10 °C.

Tensile tests were carried out for the alloys with and without vanadium with T5 and T6 (175, 250 and 325 °C) in samples that showed the maximum hardness values.

Standard cylindrical tensile specimens were machined and heat treated in an oil bath under the same conditions that the samples for hardness measurements. Specimens from the longitudinal (extrusion direction) and transverse directions were taken. Tensile tests were performed in an Instron 15 T testing machined applying a constant load of 500 k and a strain rate of (3×10^{-3} s^{-1}). Yield strength, maximum tensile strength and ductility were evaluated. Each value reported is the average value of three tests for each condition.

Fractographic analysis was carried out in fracture surfaces in the specimens that showed the highest values of mechanical properties under T5 and T6.

Results and discussion

The chemical compositions of the alloys are given in Table 2, these are within the composition range recommended by the ''Aluminum Association'' for Al6063. A slight difference in some of the minority elements between both alloys is present. For the alloy without vanadium the atomic Mg/Si ratio is 1.77, slightly lower than the stoichiometric ratio (Mg/Si = 2), this means a Si excess of 0.04 at.% and a Mg_2Si content of 0.96 at.%. For the alloy with vanadium the Mg/Si ratio is 1.098, this means an excess Si content of 0.18 at.% and Mg_2Si content of 1.13. This may be favorable to the formation of β'' hardening compound due to presence of heterogeneous nucleation sites [17, 19].

Fig. 1 shows the microstructure observed by SEM of the phases formed during casting. The typical Chinese morphology associated to the AlFeSi phase breaks up with the homogenizing treatment for both alloys. The presence of the Al_3Fe phase was also observed with a needle morphology for both alloy compositions, this phase was found more frequently in the alloy with vanadium. Figs. 2, 3, 4 show the optical micrographs for the different aging treatments and cooling rates, for the alloys with and without vanadium. The microstructural analysis does not show large differences for the different aging treatments. However, the effect of vanadium as recrystallization inhibitor is clearly observed in these micrographs and is especially significant for air and water-cooled specimens with T5 treatment. Vanadium additions restrict the growth of the recrystallized grains of the wrought alloy, resulting in a much smaller grain size for all the treatments performed. The alignment of the phases due to the extrusion process is also observed.

The identification of phases carried out by X-ray diffraction (Fig. 5) shows the presence of α-AlFeSi (cubic phase) in all the cast samples with and without vanadium. After homogenization the transformation of α-AlFeSi to β AlFeSi takes place for both alloys. The presence of these phases is associated to the slow cooling rate during solidification [21].

Transmission electron microscopy analysis carried out in the samples with and without vanadium under T5 treatment for both cooling modes (air and water), showed the presence of small round and elongated dispersoids of approximate size 0.2 μm (Fig. 6). For the samples without vanadium these precipitates were constituted mainly by Al–Fe, Al–Fe–Si and Al–Fe–Si–Mn whereas for the samples with vanadium these dispersoids also occasionally contained V, as shown in the EDS.

In the samples without vanadium with T5, air and water cooled, the formation of very fine needle-shape precipitates with an average size of 50 nm length and 7 nm of diameter, were identified as β'' phase (Fig. 7a,b). The crystallographic orientation of these precipitates is along the ⟨110⟩ and ⟨100⟩ directions for the air and water cooled samples, respectively. The

Table 2 Chemical compositions of the alloys studied (wt.%)

Element %	Si	Mg	Fe	Cu	Mn	Cr	Ti	Zn	V	Al
6063 alloy without V	0.39	0.59	0.23	0.005	0.049	–	–	0.005	–	bal.
6063 alloy with V	0.42	0.58	0.30	0.013	0.043	–	0.010	0.003	0.10	bal.

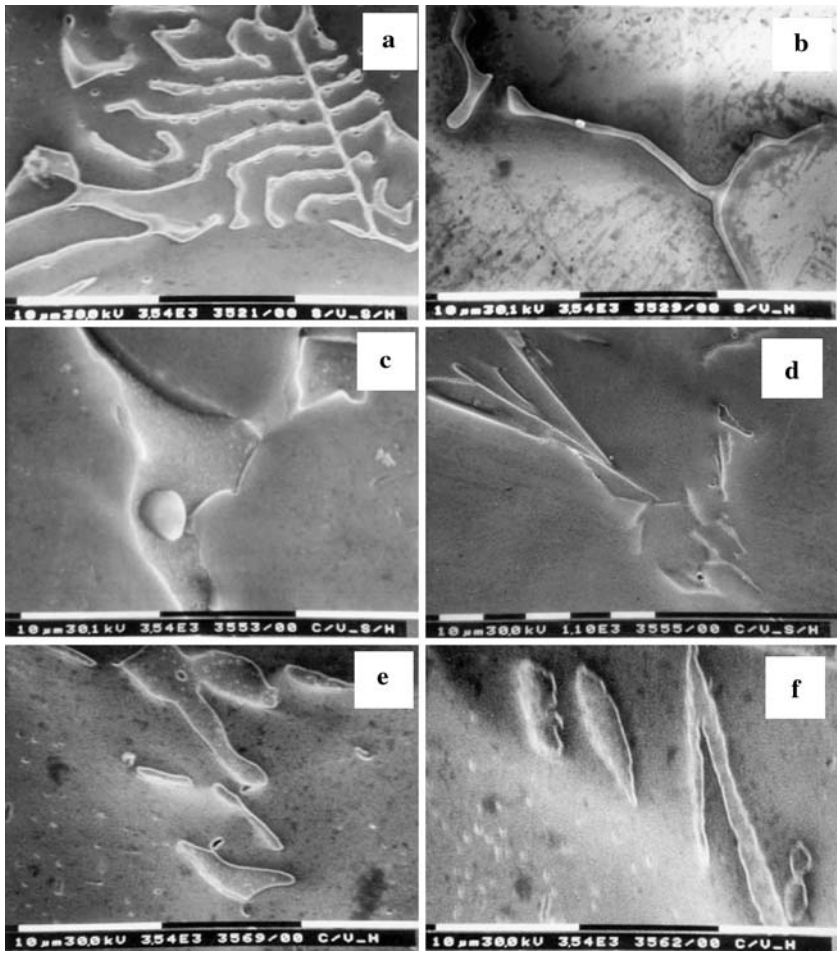

Fig. 1 SEM micrographs showing the phases present in the Al 6063 alloy without (**a**,**b**) and with vanadium (**c**–**f**): (**a**) As cast alloy showing the typical AlFeSi with Chinese script morphology. (**b**) Alloy homogenized showing the AlFeSi along the grain boundaries. (**c**) As cast alloy showing the AlFeSi phase. (**d**) As cast alloy showing the AlFe phase. (**e**) Homogenized alloy showing the AlFeSi phase. (**f**) Homogenized alloy showing the AlFe phase

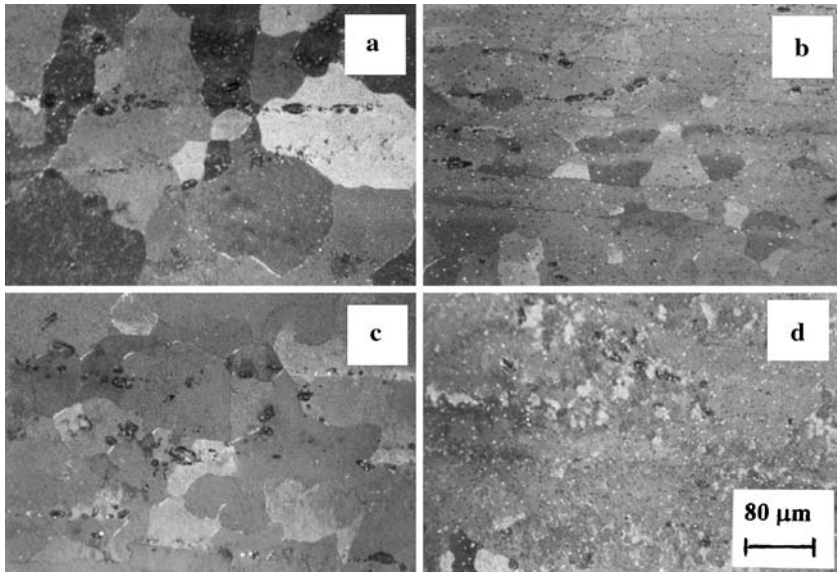

Fig. 2 Optical micrographs from extruded sections with T5 aging treatment (bar is 80 µm for all micrographs). (**a**) Alloy without air cooled. (**b**) Alloy with vanadium air cooled. (**c**) Alloy without vanadium water cooled. (**d**) Alloy with vanadium water cooled

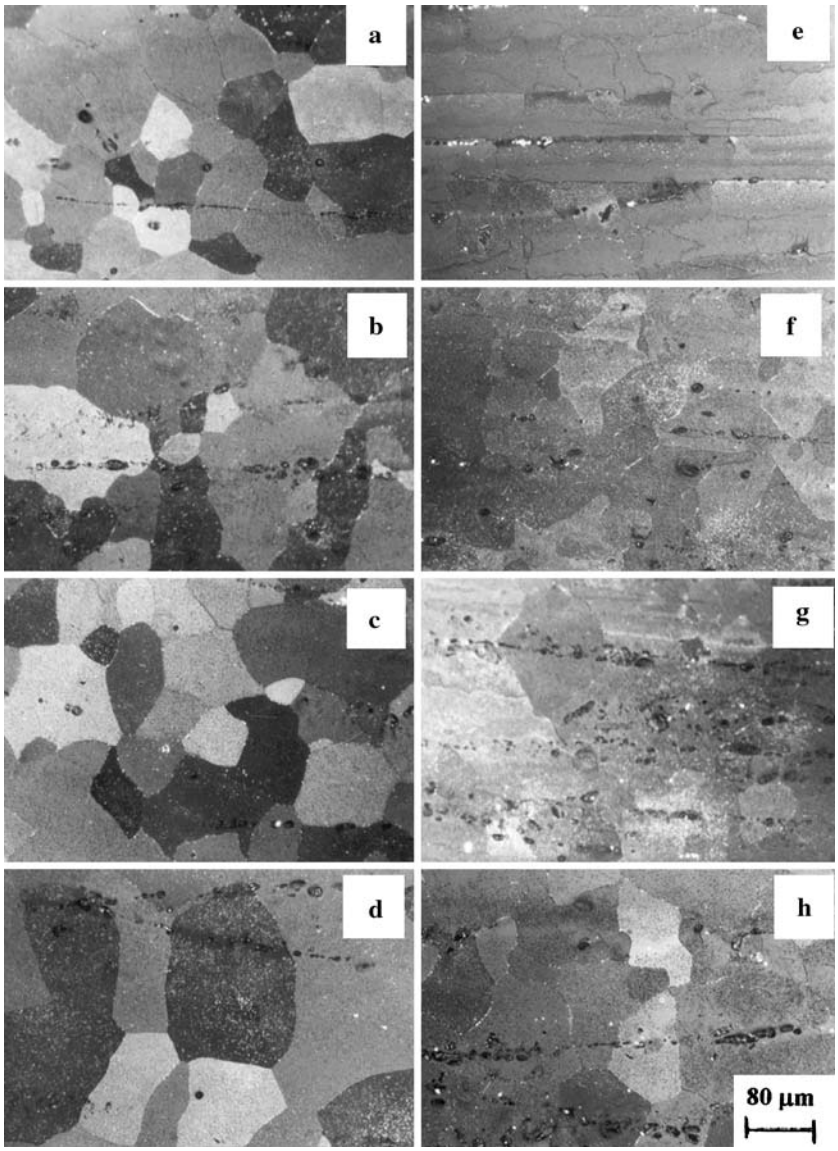

Fig. 3 Optical micrographs from extruded samples with T6-air cooled (bar is 80 μm for all micrographs). Al-6063 alloy without vanadium: (**a**) 1 h, (**b**) 8 h, (**c**) 32 h, (**d**) 128 h. Al-6063 alloy with vanadium: (**e**) 1 h, (**f**) 8 h, (**g**) 32 h, (**h**) 128 h

electron diffraction patterns showed the typical characteristic diffuse scattering due to the elastic distortions present in the matrix as a consequence of the formation of the coherent metastable β'' formation. This phase is responsible for the hardening of the Al matrix.

For the alloy with vanadium (T5) the formation of rod-shape β' precipitates, with average size of 100 nm length was observed (Fig. 7c,d) in lower density than β'' phase formed with T5. The orientation of this phase corresponds to the $\langle 100 \rangle$ directions for both cooling modes. Vanadium accelerates the kinetics of precipitation therefore β'' phase has already transformed to β' for aging at 175 °C during 8 h.

The artificial aging treatments (T6) were carried out from 1 min to 128 h at 175, 250 and 325 °C for alloys with and without vanadium, solution treated and water or air cooled.

Electron microscopy analysis of the precipitation sequence is shown in Figs. 8, 9 for alloys without and with vanadium, respectively, for aging at 175 °C for 4, 16 and 128 h water cooled. For both alloys, after aging for 4 h, the formation of β'' phase is observed.

This phase is aligned in the $\langle 001 \rangle$ orientation with an average size of 20–40 nm length and 4 nm diameter. At 16 h of aging the presence of β'' and $\beta'$are observed. The density of precipitates is high and have an average size of 60–130 nm length and 4 nm diameter. After, 128 h of aging β' still remains. This phase is oriented in the $\langle 001 \rangle$ directions and the average size is 20 nm diameter and 130–420 nm length. These observations

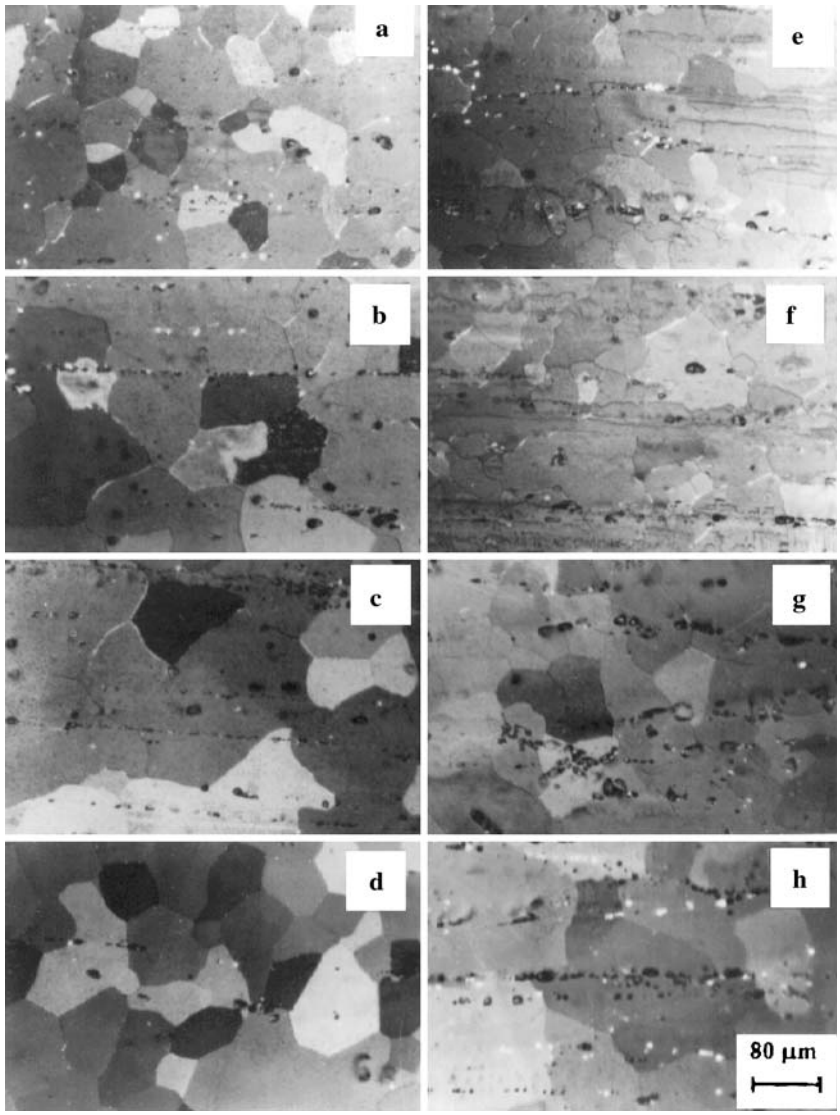

Fig. 4 Optical micrographs from extruded samples with T6-water cooled (bar is 80 μm for all micrographs). Al-6063 alloy without vanadium: (**a**) 1 h, (**b**) 4 h, (**c**) 16 h, (**d**) 128 h. Al-6063 alloy with vanadium: (**e**) 1 h, (**f**) 4 h, (**g**) 16 h, (**h**) 128 h

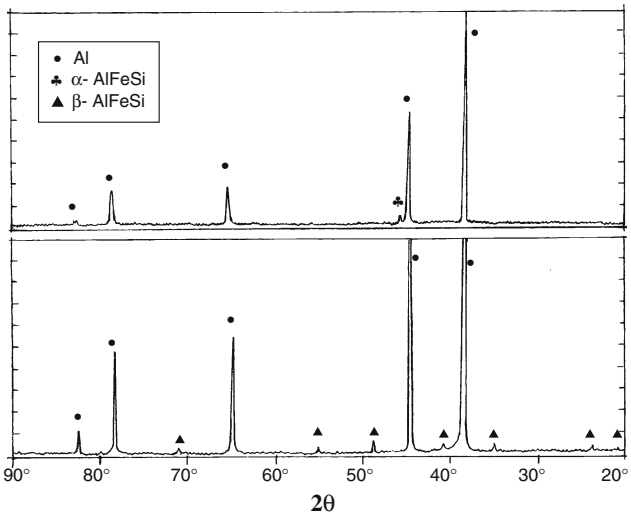

Fig. 5 Characteristic DRX of alloys with and without vanadium. (**a**) Cast and (**b**) homogenized •Al, ♣ α-AlFeSi, ▲β-AlFeSi

are consistent with the hardness values obtained. The highest value was observed for the treatment at 16 h—175 °C in which the higher density of β'' and β' precipitates were observed. For T6, alloys with and without vanadium showed a very similar behavior in precipitation sequence and size of precipitates. The presence of dispersoids was also observed for both alloys under T6 with different sizes, morphologies, compositions and crystal structures. These phases were identified as $MnAl_6$, $(Fe,Mn)Al_6$, and Al_3Fe and AlFeSi (monoclinic and hexagonal) and were found for all the aging treatments. Fig. 10 shows the typical distribution and morphology of some of these phases present in the matrix. For the alloys with vanadium some of these phases contained also V in solution, forming a phase with tetragonal crystal structure and lattice parameters of $a = 6.09$ Å, $c = 9.44$ Å. These

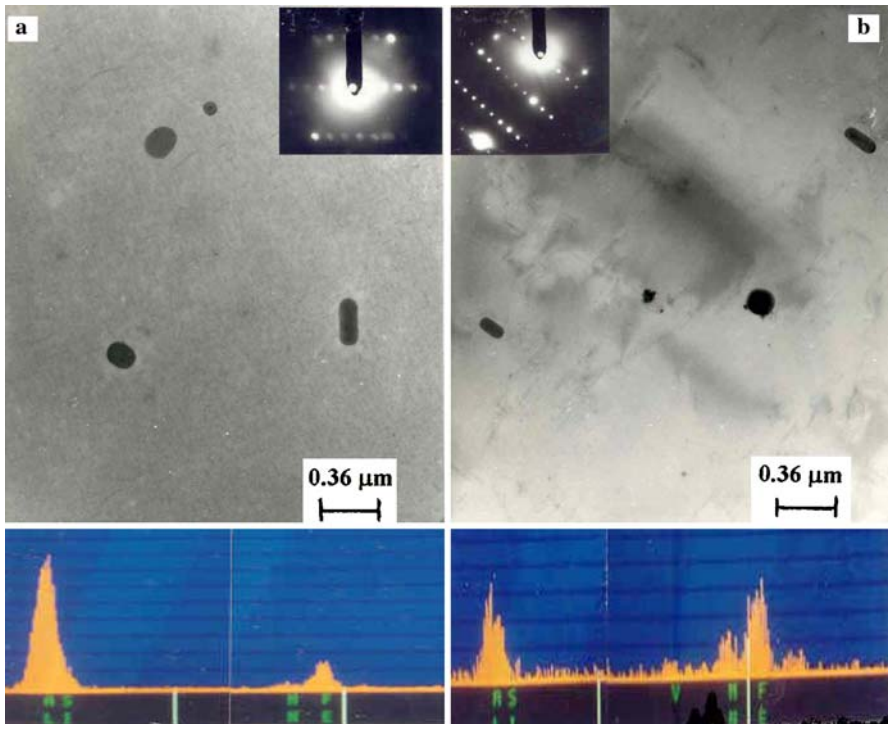

Fig. 6 TEM bright field images of dispersoids (extruded samples, T5-water cooled) showing electron diffration patterns in [120] zone axis and EDS microanalysis: (a) presence of AlFeSiMn phase in the alloy without vanadium. (b) Presence of AlFeSiMnV phase in the alloy with vanadium

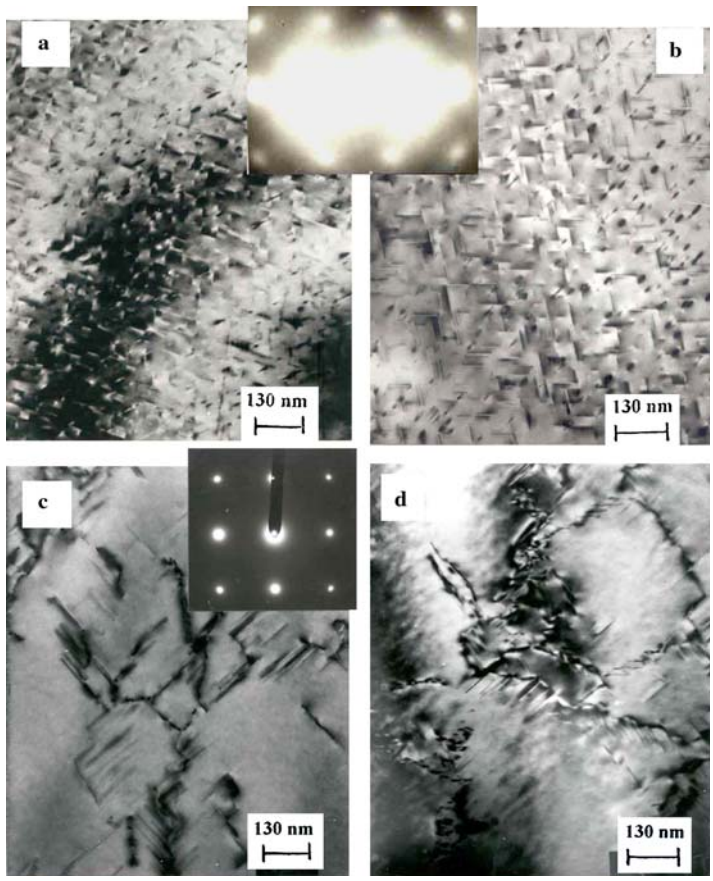

Fig. 7 TEM bright field images of samples with and without vanadium T5-water and air cooled: (**a**) without vanadium air cooled—β'', SADP B = [110], (**b**) without vanadium water cooled—β'', SADP B = [110], (**c**) with vanadium air cooled—β', SADP B = [001], (**d**) with vanadium water cooled —β'

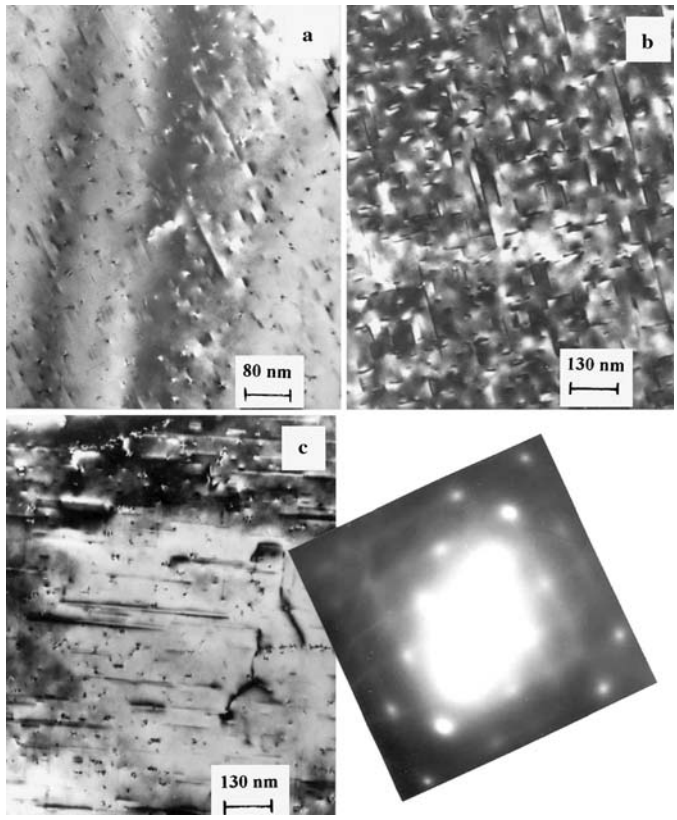

Fig. 8 TEM bright field images of the alloy without vanadium aged 4, 16 and 128 h at 175 °C: showing the electron diffraction pattern SADP B = [100]. (**a**) 4 h β'' is observed, (**b**) 16 h β' and β'' are present, (**c**) 128 h β' is present

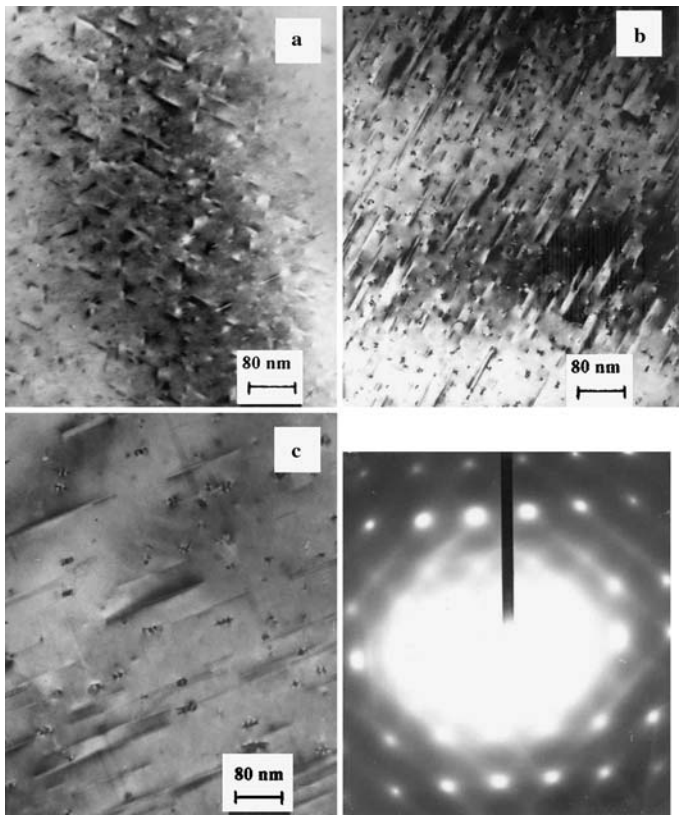

Fig. 9 TEM bright field images of the alloy with vanadium aged 4, 16 and 128 h at 175 °C: (**a**) 4 h β'' is observed (**b**) 16 h β' and β'' are present (**a**) 128 h β' is present, SADP B = [100]

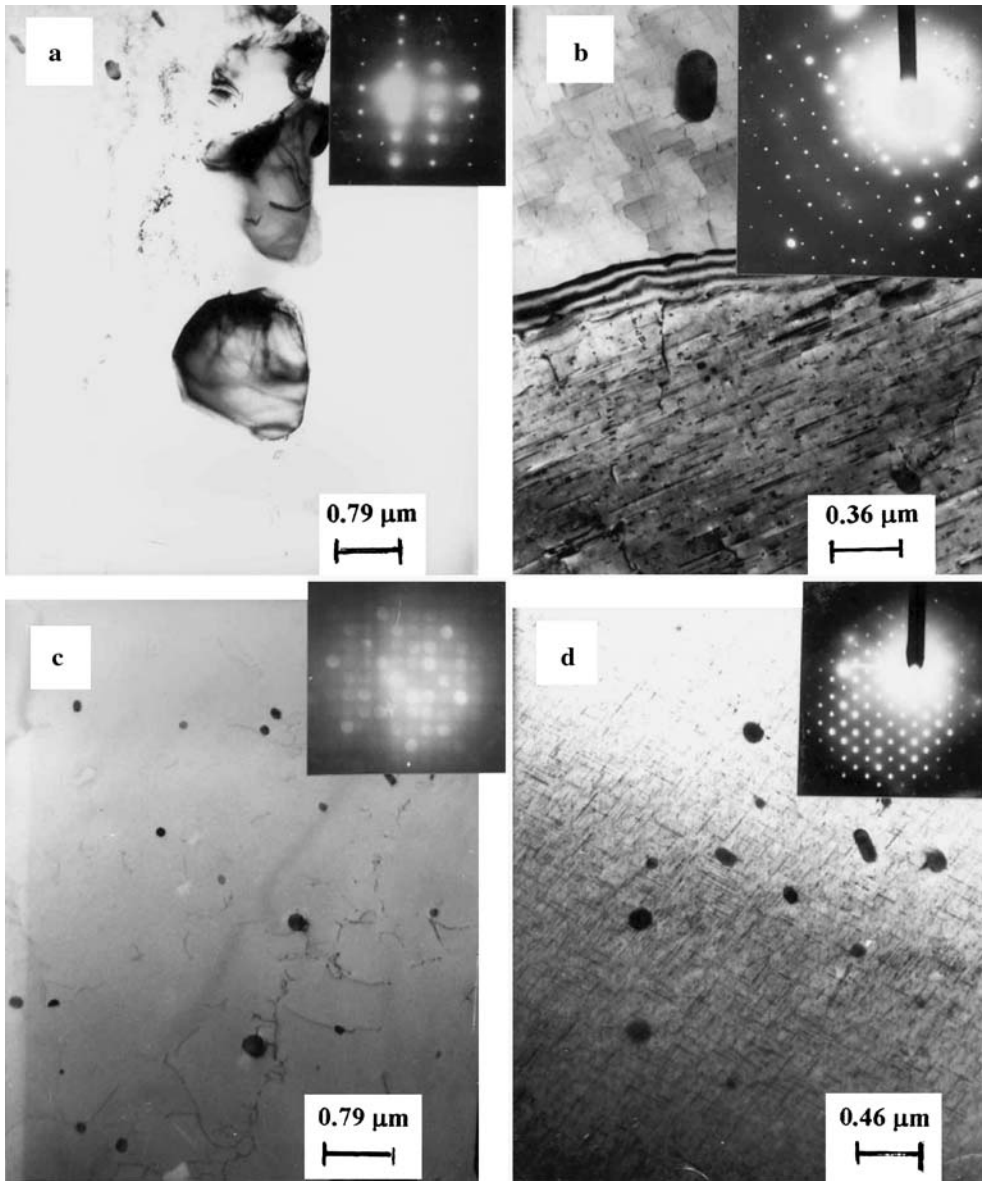

Fig. 10 TEM bright field images from extruded samples with T6-water cooled. (**a**) With vanadium T6—1 h, showing the AlFeSi-H phase, SADP B = [311], (**b**) without vanadium T6—128 h, showing the Al_3Mn phase, SADP B = [112], (**c**) with vanadium T6—1 h, showing dispersoids AlFeSiMn, SADP B = [001], (**d**) with vanadium T6—128 h, showing dispersoids of AlFeSiMnV, SADP B = [100]

dispersoids have a rounded morphology and average size of 90 nm.

Table 3 summarizes the hardness values for both alloys with T5 and T6 treatments, at the different aging temperatures and cooling modes. For T6 the hardness values shown are the maximum values observed in the curves of hardness vs. time (Fig. 11). The alloy with vanadium and T5 treatment shows lower hardness values than the alloy without vanadium for both cooling modes. This could be explained from the precipitation behavior observed in the microstructure (Fig. 7). The formation of high density of very fine needle-shape β'' phase was observed for the alloy without V (Fig. 7a,b) which is responsible for the hardening of the Al matrix. The alloy with V, for this treatment (T5), show the formation of rod-shape β' instead of β'' (see Fig. 7c,d) of larger size and in lower density than β'' precipitates observed in samples without V. Therefore, vanadium additions to Al-6063 accelerate the kinetics of precipitation of β'' and β'. This also explains the lower value of hardness observed in the samples with vanadium T5 8 h—175 °C (Table 3). This result is also consistent with the Si excess present in the alloys with V which favors the precipitation of β'', as has been reported by Matsuda et al. [17] and Muruyana et al. [19]. Therefore, both elements (Si and V) act cooperatively favoring the acceleration of the kinetics of precipitation of β'' and β'

Table 3 Hardness values for the alloys without and with vanadium heat treatment T5 and T6 (maximum values taken from Fig. 10)

The standard T5 in plant				
Sample	Modes cooling	Aging temperature (°C)	Hardness (HV)	Aging time 8 h
Without V	T5-Air	175	84.24 ± 2.72	
With V	T5-Air		43.20 ± 1.83	
Without V	T5-Water	175	84.10 ± 2.18	
With V	T5-Water		50.42 ± 1.47	
The standard T6 at laboratory scale				
Without V	Without aging		55.26	
	T6-Air	175	80.76 ± 1.39	32 h
		250	58.15 ± 0.94	1 h
		325	47.91 ± 0.51	3 min
	T6-Water	175	89.81 ± 1.74	16 h
		250	67.99 ± 1.10	27 min
		325	50.42 ± 0.66	3 min
With V	Without aging		49.36	
	T6-Air	175	71.34 ± 1.36	32 h
		250	52.39 ± 0.75	1 h
		325	43.76 ± 0.48	3 min
	T6-Water	175	89.09 ± 1.90	16 h
		250	66.76 ± 1.03	27 min
		325	55.73 ± 0.72	3 min

and maximum hardness should be obtained for shorter aging periods.

Fig. 11 shows the hardness vs. time curves, for the different temperatures (175, 250 and 325 °C), and cooling modes for both alloys with T6 treatment. As expected, as the temperature increases maximum hardness is obtained in shorter periods. The highest values are observed for the specimens with and without vanadium content, water quenched and aged at 175 °C for 16 h. In general, the samples with vanadium for this treatment show a slight decrease in hardness with respect to the samples without vanadium for the different temperatures and cooling modes, except for the treatment at 325 °C for 3 min water cooled, which shows an increase in hardness of only 11%. Alloys with and without vanadium (T6) showed a very similar behavior in precipitation sequence and size of precipitates (see Figs. 8, 9). Both alloys aged 4 h showed the formation of β'' phase, while 16 h of aging resulted in high density of β'' and β'. After, 128 h of aging the formation β' still remains. These observations are consistent with the hardness values obtained. The highest value of hardness obtained (16 h, 175 °C) was consistent with the highest density of β'' and β' observed.

Tables 4 and 5 summarizes the mechanical properties for the samples with and without V-T5 and T6, respectively. Table 5 presents the mechanical properties only of those samples that showed the maximum values of hardness. Yield strength and maximum strength are higher in alloys without V for T5 than those alloys with V. This is associated to the high density of the hardening precipitates β''. Although ductility is higher for alloys with V, this only is due to the lower strength values. In Table 5, only two conditions where V additions improve the properties can be observed, one is for water quench and aged 16 h at 175 °C, which shows only a small improvement. The other is for water quench and 3 min of aging at 325 °C in which the increase in yield strength is 45% and the increase in maximum strength is 32%, with respect to the sample without V. This can be explained by the effect of V on the acceleration of the kinetics of precipitation forming the hardening precipitates in shorter periods.

All the other conditions tested show a detrimental effect of V additions. It must be remembered that the samples tested in tensile test were only those that showed the highest hardness values. Therefore, due to the acceleration effect of V on the kinetics of precipitation, the samples tested were mainly in the β' transformation state. Therefore the mechanical properties could show an improvement for shorter aging times in which β'' would be present.

The fractographic analysis of the tested samples, with and without vanadium, with T5 and T6 treatments, both cooling modes, with the optimum mechanical properties is shown in Fig. 12a–f. The fracture surface has the typical ductile characteristics, the presence of dimples, some of them associated with AlFeSi, AlFe and AlFeMn particles, for the samples air and water cooled with and without vanadium. Schwellinger [22, 31] studying the fracture mechanisms

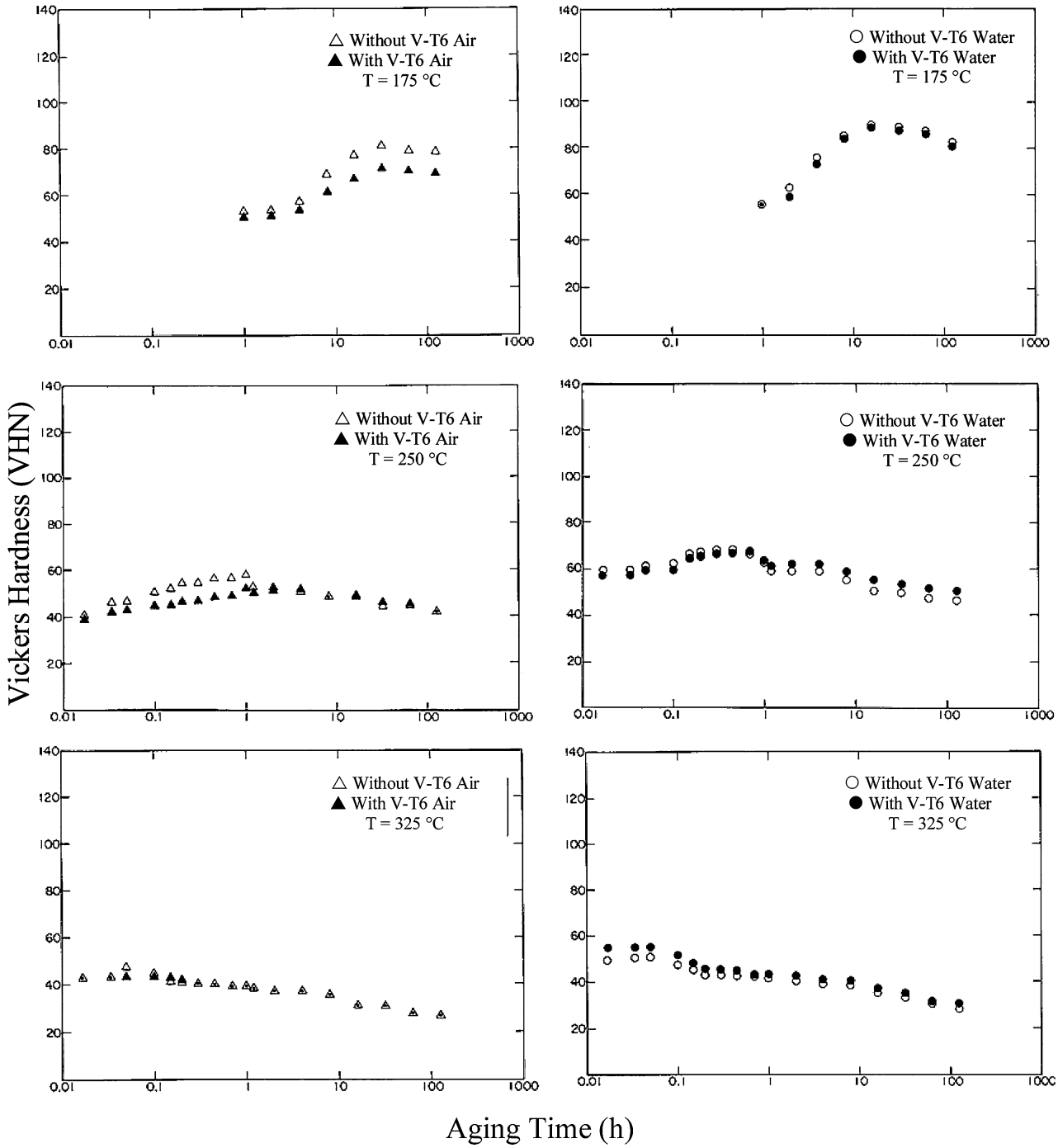

Fig. 11 Hardness–time curves for the Al 6063 alloy without and with vanadium for different temperatures (175, 250 and 325 °C) and cooling modes (forced air and water)

in Al–Mg–Si reported that the nucleation of dimples in these alloys is independent of the particles associated to the dimples when these are present in small amounts.

Conclusions

The effect of vanadium as a recrystallization inhibitor was clearly observed for both cooling modes.

Table 4 Mechanical properties for the samples without and with vanadium with T5 (aging temperature: 175 °C, aging time: 8 h, modes cooling: Air and Water)

Sample		Yield strength 0.2% (kg/cm^2)	Maximum strength (kg/cm^2)	Ductility	
				% Elongation	% Reduction in area
Without V-T5 Air	(L)	2081.54	2312.89	15.09	45.20
	(T)	1711.27	1951.26	13.24	36.65
With V-T5 Air	(L)	826.98	1278.30	27.87	63.94
	(T)	836.31	1300.55	27.41	62.60
Without V-T5 Water	(L)	1936.44	2171.13	18.80	56.58
	(T)	1774.58	2083.50	19.82	45.16
With V-T5 Water	(L)	1042.60	1473.09	17.50	59.27
	(T)	993.52	1408.12	17.78	50.04

(L) Longitudinal section
(T) Transverse section

Table 5 Mechanical properties for the samples without and with vanadium with T6 at laboratory scale

Sample		Aging temperature (°C)	Aging time	Yield strength 0.2% (kg/cm^2)	Maximum strength (kg/cm^2)	Ductility	
						% Elongation	% Reduction in area
Without V-T6-Air	(L)	175	32 h	2069.97	2288.47	13.89	29.14
	(T)			2092.51	2327.99	11.57	23.42
With V-T6-Air	(L)			2021.43	2255.66	17.41	49.33
	(T)			2032.19	2261.22	14.35	34.59
Without V-T6-Water	(L)		16 h	2075.15	2321.70	17.59	55.56
	(T)			1895.15	2142.66	14.54	49.48
With V-T6-Water	(L)			2328.47	2549.27	21.30	54.72
	(T)			2136.10	2334.07	16.85	50.92
Without V-T6-Air	(L)	250	1 h	1628.29	1911.01	10.19	61.63
	(T)			1077.06	1494.44	23.42	68.97
With V-T6-Air	(L)			1381.63	1737.95	21.30	66.04
	(T)			1308.64	1642.45	25.37	61.21
Without V-T6-Water	(L)		27 min	1794.34	2035.43	21.11	68.97
	(T)			1548.72	1806.29	20.37	63.73
With V-T6-Water	(L)			1634.98	1910.59	19.81	64.36
	(T)			1506.19	1783.75	18.15	57.02
Without V-T6-Air	(L)	325	3 min	1121.27	1523.59	22.04	72.96
	(T)			882.88	1292.87	13.34	61.00
With V-T6-Air	(L)			845.79	1302.62	26.21	69.39
	(T)			808.99	1283.02	22.50	65.41
Without V-T6-Water	(L)			902.93	1305.97	18.52	72.53
	(T)			957.95	1372.33	19.81	62.68
With V-T6-Water	(L)			1629.04	1922.33	17.96	53.67
	(T)			1027.66	1419.60	16.48	63.10

(L) Longitudinal section
(T) Transverse section

The presence of dispersoids AlFeSi, Al_3Fe, Al_6 (Fe,Mn) and $MnAl_6$ were observed in the samples without V, while for samples with V these dispersoids also occasionally contained V.

The addition of vanadium to Al-6063 alloy under T5 treatment, accelerates the precipitation kinetics of β'' and β' phase. This can also be related to the Si excess (0.18 at.%) present in the alloy with V addition favoring the formation of β''.

The precipitation sequence and size of precipitates were very similar for both alloys with T6.

All hardness values for the different aging treatments are higher in alloys without V than with V.

In general, vanadium additions have a detrimental effect on the yield strength and maximum tensile strength for the aging treatments tested.

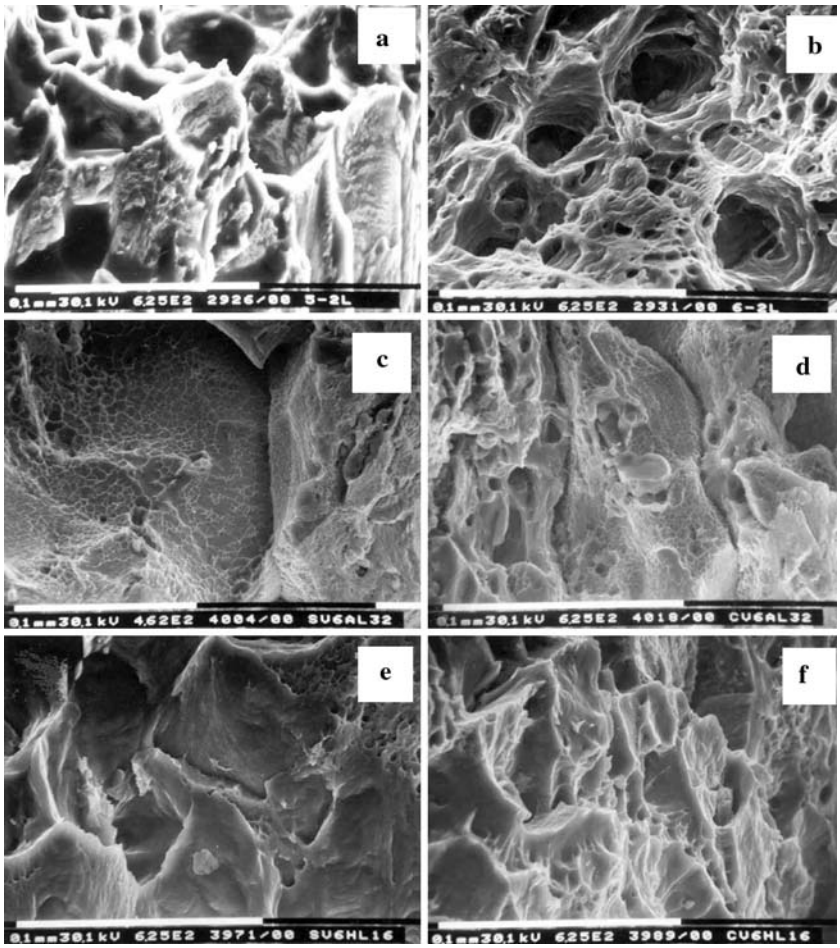

Fig. 12 SEM images of the fracture surfaces of tested samples that showed optimum mechanical properties. (**a**) Alloy without vanadium, T5 aged 16 h water cooled. (**b**) Alloy with vanadium, T5 aged 16 h water cooled. (**c**) Alloy without vanadium, T6 aged 32 h air cooled. (**d**) Alloy with vanadium, T6 aged 32 h air cooled. (**e**) Alloy without vanadium, T6 aged 16 h water cooled. (**f**) Alloy with vanadium, T6 aged 16 h water cooled

References

1. Aluminum Standards and Data 1979, 6th ed. The Aluminum Association, March, 1979
2. Evans DW, Aucote J (1984) Proceedings of the Third International Aluminum Extrusion Technology Seminar, vol 1, p 53
3. Ohuri K, Takeuchi Y, Matsuyama H (1984) Proceedings of the Third International Aluminum Extrusion Technology Seminar, vol 1, p 63
4. Blade C, Bryant J, Thomas T (1976) Met Tech August: 380
5. Thomas G (1961–1962) J Inst Metals 90:57
6. Kelly A, Nicholson RB (1963) Prog Mater Sci 10:152
7. Pashely DW, Jacobs MH, Vietz JT (1967) Philos Magn 16:51
8. Jacobs MH (1972) Phil Mag 26:1
9. Kovacs I, Lendvai J, Nagy E (1972) Acta Met 20:975
10. Lorimer GW (1976) In: Russell KC, Aaronson H (ed) Conf. Proceed. The Metall. Soc. AIME
11. Katz Z, Ryum N (1981) Scripta Metall 15:265
12. Lynch JP, Brown LM, Jacobs MH (1982) Acta Metall 30:1389
13. Dutta I, Allen SM (1991) J Mater Sci Lett 10:323
14. Takeda M, Ohkubo F, Shirai T, Fukui K (1998) J Mater Sci 33:2385
15. Edwards GA, Sfillers A, Dunlop GL, Couper MJ (1998) Acta Metall 48(11):3893
16. Matsuda K, Naoi T, Fujii K, Uetani Y, Sato T, Kamio A, Ikeno S (1999) Mater Sci Eng A262:232
17. Matsuda K, Sakaguchi Y, Miyata Y, Uetani Y, Sato T, Kamio A, Ikeno S (2000) J Mater Sci 35:179
18. Ringer SP, Hono K (2000) Mat Character 44:101
19. Muruyana M, Hono K (1999) Acta Mater 47(5):1537
20. Ohmori Y, Chau Doan L, Matsuura Y, Kobayashi S, Nakai K (2001) Mater Trans 42(12):2576
21. Tanihata H, Sugawara T, Matsuda K, Ikeno S (1999) J Mater Sci 34:1205
22. Schwellinger P (1979) Scripta Metall 13(6):497
23. Zhen L, Kang SB (1998) Mater Lett 37:349
24. Panseri C, Federighi T (1966) J Inst Metals 94:99
25. Bowden DW (1984) J Metals 36(12):25
26. Evans DW, Aucote J (1984) Proceedings of the Third International Aluminum Extrusion Technology Seminar, Atlanta, vol 1, p 53
27. Lodgaard L, Ryum N (2000) Mater Sci Eng A283:144
28. Schwellinger P, Zoller H, Maitland (1984) Proceedings of the Third International Aluminum Extrusion Technology Seminar, Atlanta, vol 1, p 17
29. Babic E, Girt E, Kasnic R, Leontic B, Occko M, Vucic Z, Zoric I (1973) Phys Stat Solid (a) 16:K21
30. Mondolfo LF (1976) Aluminum alloys: structure and properties. Buttherworths, London
31. Schwellinger P (1980) Scripta Met 14(7):769